THz Integrated Circuit with a Pixel Array to Multiplex Two 10-Gbit/s QPSK Channels Each on a Different OAM Beam for Mode-Division-Multiplexing

Xinzhou Su[1]*, Hao Song[1], Huibin Zhou[1], Kaiheng Zou[1], Yuxiang Duan[1], Narek Karapetyan[1], Runzhou Zhang[1], Amir Minoofar[1], Haoqian Song[1], Kai Pang[1], Shlomo Zach[2], Andreas F. Molisch[1], Moshe Tur[2], and Alan E. Willner[1]

1. Depart. of Electrical Engineering, University of Southern California, Los Angeles, CA 90089, USA. Email: xinzhous@usc.edu

2. School of Electrical Engineering, Tel Aviv University, Ramat Aviv 69978, ISRAEL

Abstract: We design and fabricate a pixel-array-based THz integrated circuit for the generation and multiplexing of multiple OAM beams. We experimentally demonstrate a 20-Gbit/s QPSK free-space THz link at 0.317 THz by multiplexing OAM +1 and –1 using the integrated circuit.

1. Introduction

Terahertz (THz) systems are gaining interest for free-space wireless communication links due to their: (a) higher bandwidth and lower beam divergence when compared to millimeter waves, and (b) lower degradation due to atmospheric turbulence when compared to optical waves [1-3]. Moreover, the 300-GHz region is particularly low in power absorption and turbulence effects [1]. There are multiple examples of free-space THz communication links that transmit a single Gaussian beam from the transmitter to the receiver [4-6].

Similar to communication systems in other frequency ranges, there have been advances in THz links to increase system capacity by multiplexing multiple independent data-carrying beams at the transmitter, transmitting them over the same free-space medium, and demultiplexing them at the receiver [4, 5, 7]. An example is mode-division-multiplexing (MDM), which is a subset of space-division-multiplexing (SDM), in which each THz beam has a different spatial modal structure that is orthogonal to all other beams [7, 8]. One type of modal basis set is orbital-angular-momentum (OAM), which is a subset of Laguerre Gaussian modes [8-10]. In this case, each beam has a different OAM value of ℓ, such that ℓ is the number of 2π phase changes in the azimuthal direction and the intensity profile is a vortex [9, 10].

Key advances in optical systems include the use of photonic integrated circuits (PIC) in order to improve performance (e.g., cost, size, weight, and power consumption) [2, 11]. It seems appropriate that THz integrated circuits (TIC) would likewise bring significant value to THz communication systems [2]. Recent work of OAM-THz integration work includes: (a) a metasurface that converts a free-space Gaussian beam into a free-space OAM beam but without any data transmission [12], and (b) a chip that generates a single tunable OAM beam carrying ~Mbit/s OAM-encoded data [13]. However, a laudable goal might be to have a THz integrated circuit that generates multiple OAM beams, multiplexes them together for transmission of high-speed data (>Gbit/s).

In this paper, we experimentally demonstrate a THz integrated circuit with a pixel array capable of multiplexing two 10-Gbit/s quadrature-phase-shift-keying (QPSK) channels each on a different OAM beam for MDM. We design and fabricate a THz silicon integrated circuit with an OAM mode converter that can vertically emit and multiplex OAM +1 and –1 with the signals from the left and right input ports, respectively. The crosstalk between two modes is less than –15 dB at the center frequency of 317 GHz. The device has a 3-dB bandwidth of ~15 GHz, and the crosstalk is <–10 dB within this band. In total, 20 Gbit/s data rate is achieved for a THz free-space multiplexed OAM link.

2. Concept and experimental setup

As shown in Fig. 1(a), the THz integrated OAM emitter has two input ports that couple THz signals from the hollow metallic waveguides to the silicon waveguides. The OAM mode converter at the center of the device has a pixel array structure and can vertically couple/emit coaxially-propagated OAM +1 and –1 modes to the free-space with TE_{00} input waveguide mode from the left and right ports, respectively. Two emitted OAM modes have the same linear polarization. This THz integrated circuit is made out of a 200-μm silicon slab waveguide, and some of the pixels inside the OAM converter are partially etched with a 60-μm depth. Figure 1(b) shows the schematic diagram of the integrated device. The device mainly consists of three regions. (i) two coupling spikes serve as the input ports, which can be inserted into WR3.4 hollow metallic waveguides and couple THz waves from the waveguides with relatively low coupling loss [14]. (ii) Two adiabatic tapering structures surrounded by effective medium cladding with waveguide size from 280 μm to 3.6 mm to expand the mode profile, while remaining the modal structure as a single TE_{00} mode. The simulated intensity of the electrical field inside the tapering structure is shown in the inset of Fig. 1(b). The effective medium is made of periodic dense hollow lattice, and functions as the low-refractive-index cladding and mechanical supporting frame of the circuit [14]. The refractive index of silicon is 3.417 and the designed index of the effective medium is 1.6. (iii) Pixel-array-based OAM mode converter that can vertically emit and multiplex two OAM modes into the free-space with inputs from two different ports. The OAM mode converter has a size of 3.6×3.6 mm. The simulated far-field intensity and phase profiles of the generated OAM +1/–1 are shown in Fig. 1(b).

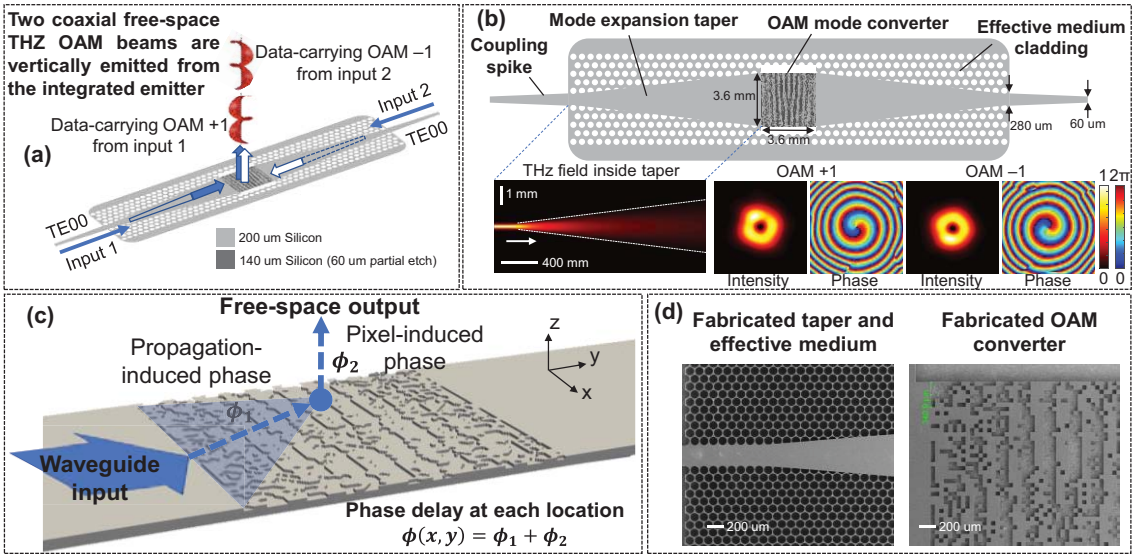

Figure 1. (a) Concept of pixel-array-based THz integrated OAM emitter. (b) Schematic diagram of the integrated OAM emitter and simulated beam profiles of mode inside the taper structure and far-field of the generated OAM +1/–1 beam. (c) Concept of OAM mode converter vertically emits different spatial modes from different waveguide inputs. (d) Scanning electron microscopy pictures of the fabricated device.

The concept of the pixel-array-based OAM converter is illustrated in Fig. 1(c). The phase profile of the vertically emitted beam at different locations is jointly controlled by the path length and different pixels at different locations. In general, the resulting phase delay at each location $\phi(x, y)$ composes both the propagation-induced phase ϕ_1 and the pixel-induced phase ϕ_2 (the pixel type is determined by the area with or without partial etch). By utilizing an optimization algorithm to design the distribution of the pixels, the spatial distribution of the THz phase profile can be jointly controlled with a term of $\phi = \ell\theta$ [15]. θ represents the azimuthal angle. It should be noted that such a pixel-array-based OAM converter could be designed and extended with more inputs and outputs, and the generated OAM mode order could be tuned if a phase shifter is designed for each input port [16]. Figure 1(d) shows the scanning electron microscopy (SEM) pictures of the fabricated tapering structure, effective medium cladding, and OAM converter (fabricated by Microfluidic Foundry).

Figure 2(a) represents the experimental setup. At the transmitter, the output of Laser 1 is modulated with a 5-Gbaud QPSK signal and combined with a continuous-wave (CW) light from Laser 2. The frequency spacing between the two lasers controls the carrier frequency of the generated THz signal $f_{THz} = \Delta f$, and is set to be ~300 GHz. The combined signal is split into two paths and one of the paths is delayed by a 15-m fiber for decorrelation. For each path, the combined data signal and CW light are mixed in a positive-intrinsic-negative photodiode (PIN-PD) based THz Gaussian emitter to generate THz data signal in free-space. The free-space THz signal is coupled into a WR3.4 metallic waveguide by two horn antennas. Subsequently, the THz integrated circuit generates two coaxially-propagated OAM +1 and OAM –1 beams with the inputs from left and right ports connected to the antennas. The multiplexed OAM beams are converted back to a Gaussian beam one at a time using a spiral phase plate [7]. The back-converted THz beam is collected by a horn antenna, subsequently amplified by a THz amplifier, and down-converted to intermedia frequency (IF) band by beating with a 12-times frequency multiplied radio frequency (RF) signal from the electrical local-oscillator (LO) in a THz sub-harmonic down converter ($f_{IF} = f_{THz} - 12 \times f_{LO}$). The IF signal is sampled by a digital oscilloscope and demodulated by offline postprocessing.

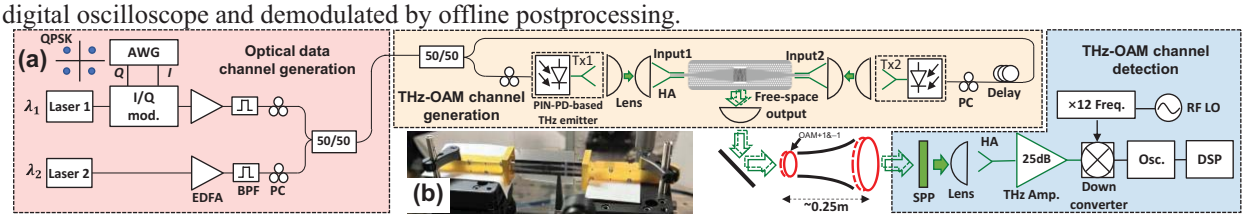

Figure 2. (a) Experimental setup of a 20-Gbit QPSK THz OAM-multiplexed links using two OAM beams generated and multiplexed by a THz integrated OAM emitter at 0.317 THz. (b) Picture of the fabricated THz integrated OAM emitter inserted into two horn antennas with WR3.4 hollow metallic waveguide. AWG: Arbitrary Waveform Generator; EDFA: Erbium-Doped Fiber Amplifier; BPF: Band Pass Filter; PC: Polarization Controller; SPP: Spiral Phase Plate; BS: Beam Splitter; HA: Horn Antenna; Osc.: Oscilloscope; DSP: Digital Signal Processing.

3. Experimental results and discussion

To characterize the generated OAM beams generated by the THz integrated OAM emitter, we first transmit a CW THz wave, and measure the intensity profile of the generated OAM beams and the interferogram with a Gaussian

beam, as shown in Fig. 3(a). The number of rotating arms and the rotating direction (clockwise or counterclockwise direction) shown in the interferograms corresponds to the mode order of the relevant OAM beams and their signs. The intensity profiles of back-converted Gaussian beams are also measured using corresponding SPPs to back convert the OAM beams. We also measure the modal spectrum of the generated OAM +1/ –1 beams at the center frequency of the device ~317 GHz by changing the OAM order of the SPP at Rx. As shown in Fig. 3(b), the power leaked to neighboring modes is ~ –11 dB and ~ –9 dB for OAM +1 and –1, respectively. With a similar method, we measure the normalized received power of OAM +1/–1 modes when transmitting OAM +1/–1 at different frequencies. It shows that the 3-dB power bandwidth of the device is ~15 GHz, and the crosstalk between OAM +1/–1 channels can be remained <–10 dB within this band.

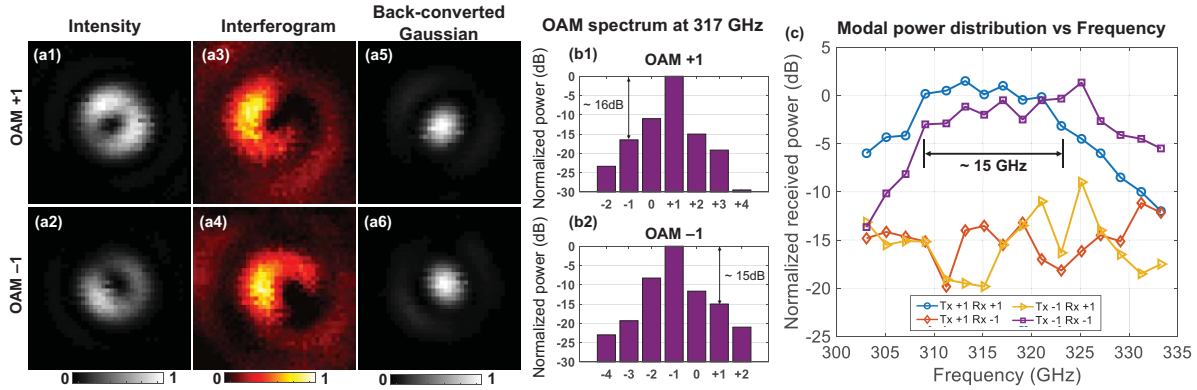

Figure 3. (a1, 2) Intensity profiles, (a3, 4) interferogram with a THz Gaussian beam, and (a5, 6) back-converted Gaussian beam for the generated OAM +1/–1 by the THz integrated OAM emitter. (b1, 2) Modal spectra for OAM +1 and OAM –1 beams at the center frequency of the device ~317 GHz. (c) modal power distribution at the different frequencies ranging from 303 GHz to 333 GHz.

Experimental results of the data transmission using the THz integrated OAM emitter are shown in Fig. 4. We first measure the normalized received power of two multiplexed OAM +1/–1channels. The results in Fig. 4(a) show a ~ –16-dB modal crosstalk between OAM +1 and OAM –1 at 317 GHz. Subsequently, a 20-Gbit/s QPSK free-space THz link (5 Gbaud per channel) is demonstrated. Figures 4(b, c) show the optical spectra at Tx and the electrical spectra after down-conversion to ~11 GHz at the Rx. Figure 4(d) shows the bit error rate (BER) performance of OAM +1/–1 channel at different signal-to-noise ratios (SNR) with single-channel/multiplexed channels transmitted when using the THz integrated OAM emitter. For the THz multiplexed OAM link, the crosstalk from different OAM data-carrying channels would induce ~1 dB SNR penalties at the 7% forward error correction (FEC) threshold. The corresponding constellations and measured error vector magnitude (EVM) for single/multiplexed data channels at the SNR ~11 dB are shown in Fig. 4(e).

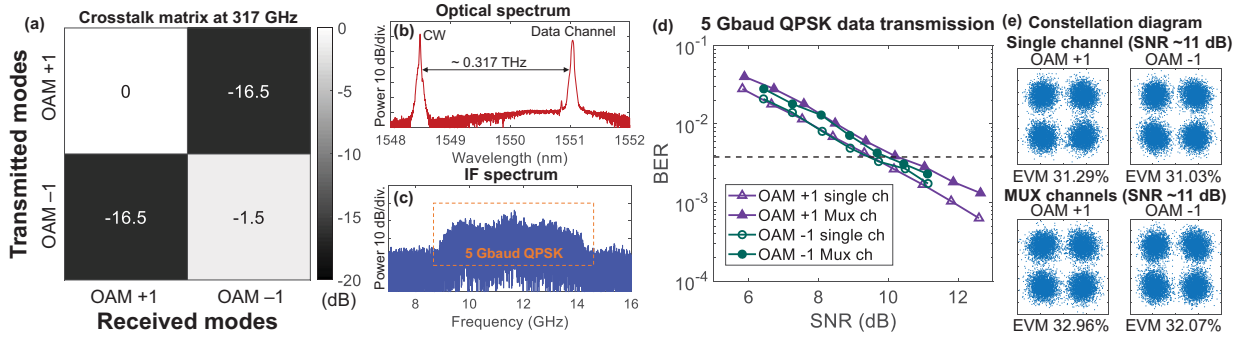

Figure 4. (a) Channel crosstalk between two multiplexed OAM channels generated by the THz integrated emitter. (b) The optical spectrum at the THz transmitter. (c) Electrical spectrum after down conversion at the receiver. (d) Measured BER as a function of SNR for two multiplexed OAM channels with a 5-Gbaud QPSK signal. (e) The EVMs and constellation diagrams under an SNR of ~11 dB.

Acknowledgment

Generous Support from VBFF through ONR (N00014-16-1-2813); Defense Security Cooperation Agency (DSCA 4440646262); Airbus Institute for Engineering Research; DURIP (FA9550-20-1-0152); Qualcomm Innovation Fellowship.

References

[1] T. Nagatsuma et al., Nat. photonics, 10(6), (2016). [2] K. Sengupta et al., Nat. Electron., 1(12), (2018). [3] K. Su et al., J. Opt. Soc. Am. A., 29(11), (2012). [4] S. Koenig et al., Nat. photonics, 7(12), (2013). [5] T. Nagatsuma et al., Opt. express, 21(20), (2013). [6] T. Harter et al., Nat. Photonics, 14(10), (2020). [7] H. Zhou et al., CLEO STh2F. 7. (2021). [8] J. Wang et al., Nature Photonics 6(7), (2012). [9] A.M. Yao et al., Adv. Opt. Photonics, 3(2), (2011). [10] L. Allen et al., Phys. Rev.A, 45(11), (1992). [11] M. Smit et al., Laser Photonics Rev., 6(1), (2012). [12] C. Zheng et al., Adv. Opt. Mater., 9(10), (2021). [13] MIW. Khan et al., IEEE J. Solid-State Circuits, (2022). [14] D. Headland et al., J. Light. Technol., 38(24), (2020). [15] Z. Xie et al., Light: Sci. Appl., 7(4), (2018). [16] H. Song et al., Opt. Lett., 46(19), (2021).